

## Pure-shift IMPRESS EXSIDE – Easy measurement of $^1\text{H}$ - $^{13}\text{C}$ scalar coupling constants with increased sensitivity and resolution.

Ikenna E. Ndukwe and Craig P. Butts\*

School of Chemistry, University of Bristol, BS8 1TS, United Kingdom.

### Supporting Information

#### Experimental

All experiments were run with a freshly prepared 30 mg sample of strychnine or menthol dissolved in 0.7 ml  $\text{CDCl}_3$  on a Varian VNMRs 500 MHz Direct Drive Spectrometer with Agilent OneNMR probe. The NMR experiments were acquired at 25°C. The inter-pulse delay,  $\tau$ , during the INEPT periods were optimized for  $^nJ_{\text{CH}} = 8$  Hz. Data were collected with  $^1\text{H}$  and  $^{13}\text{C}$  spectrum widths of 10,000 Hz and 629.5 Hz respectively and centred at 5.0 ppm in  $F_2$ . Four scans of 1600 complex points were also collected for each  $t_1$  increment of a total of 42, with zero-filling to  $4096 * 8192$  ( $t_1 * t_2$ ) after linear prediction to 84 complex points along the  $F_1$  dimension. A  $J$  scaling factor,  $N$ , of 15 was used in these experiments giving an average experimental run time of 12.5 minutes, 50 minutes and 55 minutes for SeEXSIDE, ImpEXSIDE and ImpEXSIDE\_PS respectively. All data were collected with a recovery delay of 1 second and the data obtained were processed with an unshifted Gaussian window function along both  $F_1$  and  $F_2$  dimensions. The ImpEXSIDE and ImpEXSIDE\_PS data were acquired with four band/region selection in  $F_1$  (that is four  $^{13}\text{C}$  chemical shifts). The chemical shift range of the first selected  $^{13}\text{C}$  region is set such that the peaks in the other three regions are aliased away from the  $F_1$  edges of the first region. We have used the same  $F_1$  spectrum width (629.5 Hz) for all four regions for ImpEXSIDE and ImpEXSIDE\_PS data used in this paper. Two multiple frequency shifted laminar  $wurst2i$   $^{13}\text{C}$  pulses (shown in red as  $S_1$  and  $S_2$  in ImpEXSIDE sequences, Figure S1 and Figure S2) or single frequency shifted laminar  $wurst2i$   $^{13}\text{C}$  pulses (shown in red in SeEXSIDE sequence, Figure S3) of duration  $\approx 31.84$  ms were used throughout this work. Complete selectivity is ensured by the use of the dephasing/rephasing gradients 'A' and 'B' of length 1.0 ms and power, 8531 and 1280 dB respectively. As mention, a  $J$ -scaling factor, 15, was used in these experiments. This value, however, can be increased to improve the resolution of the peaks in  $F_1$ , further revealing small couplings while providing more accurate measurement of  $^nJ_{\text{CH}}$  values but with loss of signal owing to the increased length of time of the selective INEPT-type preparation period,  $\tau + \Delta$  (where  $\Delta = t_1 * J -$

scaling factor and  $\tau = 1/(2 * {}^n J_{CH})$ ). The length of data acquired per chunk,  $\mathbf{at/n}$  (herein referred to as chunkwidth), during the windowed acquisition period of the ImpEXSIDE\_PS sequence (Figure S2) is 0.008 ms for all experiments, but can be modified as required but with a compromise between resolution and increased artifacts. This value is however limited to  $< 1/(3 * {}^n J_{HH})$  to minimize breakthrough of homonuclear coupling. It should be noted that the total acquisition time,  $\mathbf{at}$  is an integer multiple of the chunkwidth and is 0.16 s throughout this work. The gradients Ca and Cb are 500  $\mu$ s long with power 250 and 375 dB respectively with Ca either side of a hard  $180^\circ$   ${}^1\text{H}$  pulse and Cb either side of a selective  $180^\circ$  (RSNOB)  ${}^1\text{H}$  pulse. Detailed description of the ImpEXSIDE pulse sequence follows below.

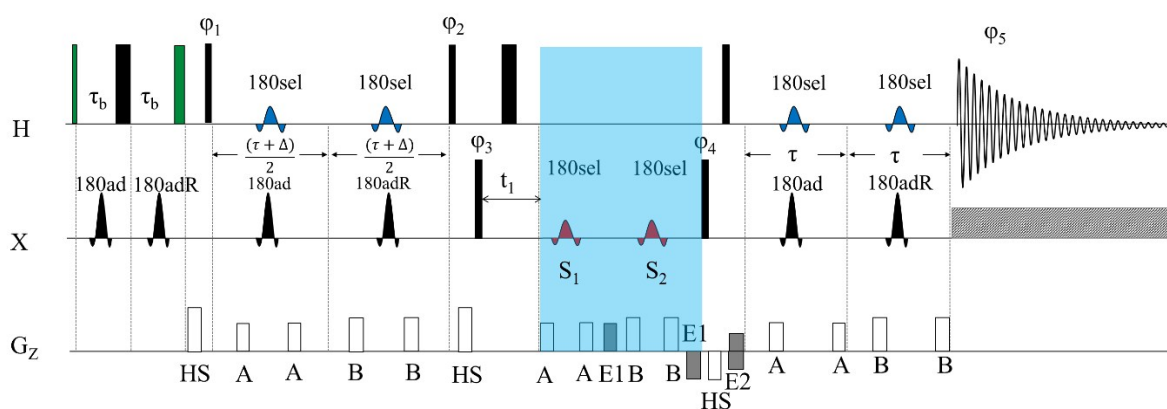


Figure S1: ImpEXSIDE pulse sequence. Wide and narrow filled boxes represent  $180^\circ$  and  $90^\circ$  pulses respectively while thick and slim green boxes are  $135^\circ$  and  $45^\circ$  pulses respectively. Shaped pulses are  ${}^1\text{H}$  selective q3 (blue),  ${}^{13}\text{C}$  selective wurst2i (red) and broadband adiabatic (black) pulses. Delays are set thus;  $\tau = 1/(2 * {}^n J_{CH})$ ,  $\tau_b = 1/(2 * {}^1 J_{CH})$ , and  $\Delta = t_1 * J - \text{scaling factor}$ . Where  ${}^n J_{CH} = 8 \text{ Hz}$ ,  ${}^1 J_{CH} = 146 \text{ Hz}$  and  $J = 15$  in this instance. The phase cycle are;  $\phi_1 = x, x, -x, -x$ ,  $\phi_2 = y$ ,  $\phi_3 = x, -x$ ,  $\phi_4 = x, x, x, x, -x, -x, -x, -x$ ,  $\phi_5 = x, -x, -x, x, x, x, -x$ . Pulses whose phases are not shown have an  $x$  phase. The pulse field gradients are shown in the  $G_z$  line as rectangular filled and unfilled boxes and coherence selection for desired  ${}^1\text{H} - {}^{13}\text{C}$  correlation is achieved with 1.0 ms encoding/decoding gradients, E1:E2 whose power is set to 1.99:1 (1067:536.29 dB in this case). HS is a 1.0 ms homospoil gradient of power, 6180 dB which causes rapid relaxation of transverse magnetization present. Gradients 'A' and 'B' are 1.0 ms frequency dephasing/rephasing gradients of power 8531 and 1280 dB respectively. The  ${}^{13}\text{C}$  band selective pulses,  $S_1$  and  $S_2$  (wurst2i pulses) can simultaneously and efficiently excite multiple frequencies. The duration of the  $90^\circ$  pulse was 9.8  $\mu$ s (power, 58 dB) and 9.0  $\mu$ s (power, 54 dB) for  ${}^1\text{H}$  and  ${}^{13}\text{C}$  nuclei respectively. The adiabatic  ${}^{13}\text{C}$   $180^\circ$  pulses (denoted 180ad and 180adR) are wurst2i swept pulse of duration 465.5  $\mu$ s and power 48 dB.

The ImpEXSIDE sequence, starts with a TANGO train [ $45^\circ_x - \tau_b - 180^\circ_x ({}^1\text{H}/{}^{13}\text{C}) - \tau_b - 135^\circ_x$ ] for one-bond ( ${}^1 J_{CH}$ ) suppression by selective excitation of protons directly bonded to  ${}^{13}\text{C}$ . The phase cycle on the first  $90^\circ$  proton pulse (which produce transverse magnetization) removes direct responses to  ${}^{12}\text{C}$ . The resultant transverse magnetization is then selectively transferred to the coupled  ${}^{13}\text{C}$  using a selective INEPT-type coherence transfer block modified by the use of the Double Pulse Field Gradient Spin Echo (DPFGSE) mechanism [ $90^\circ_x - (\tau + \Delta)/4 - G_1 - 180^\circ_x ({}^1\text{H}/{}^{13}\text{C}) - G_1 - (\tau + \Delta)/2 - G_2 - 180^\circ_x ({}^1\text{H}/{}^{13}\text{C}) - G_2 - (\tau + \Delta)/4 - 90^\circ_x$ ]<sup>20</sup> and the first  $90^\circ$   ${}^{13}\text{C}$  pulse. Multiple proton resonances can be selectively transferred to their coupled  ${}^{13}\text{C}$  with the DPFGE pulse train as long as they are not coupled to each other. This ensures that only  ${}^1\text{H} - {}^{13}\text{C}$  coupling evolves during this period while  ${}^1\text{H} -$

$^1\text{H}$  coupling to non-selected protons is refocused. The symmetrically shifted  $^{13}\text{C}$   $180^\circ$  wurst2i inversion pulses ( $S_1$  and  $S_2$ ) applied as a DPFGE element and placed after the  $t_1$  period serves to, (i) phase-encode the  $^{13}\text{C}$  frequencies (chemical shifts) of interest in the fashion of Hadamard matrix,  $H_n$  (where  $n = 4$  in this instance. See below for a  $H_4$  matrix and the main paper for full description of how it is applied in the IMPRESS element) and (ii) re-phase chemical shift and  $^1\text{H} - ^{13}\text{C}$  scalar coupling evolution. The magnetization is then back-transferred to the  $^1\text{H}$  spins where in-phase signals is then observed at the end of the selective reverse-INEPT-type element.

Further sensitivity and resolution is achieved with the ImpEXSIDE\_PS sequence (shown in Figure S2) by homonuclear decoupling in the detected dimension using an interleaved acquisition and band selective  $J -$  refocusing element highlighted in Figure S2. The preparation, evolution and mixing periods, including the pulse phases and phase cycle, are the same as the ImpEXSIDE sequence (discussed above). The windowed acquisition period is hence described. This period consists of  $n -$  repeating units of acquisition data chunk of length,  $at/n$  and  $J -$  refocusing element (comprising of a hard  $180^\circ$  and a selective  $180^\circ$   $^1\text{H}$  pulses) which serves to re-phase homonuclear scalar coupling as well as chemical shift evolution of the active spins as long as only non-mutually coupled spins are selected. The  $^1\text{H}$  selective pulse (green in Figure S2) during the windowed acquisition period should be short so as to minimize artefacts/sidebands arising from regular discontinuities in the intensity of data points where the FIDs is 'stitched' back together. The duration of the  $J -$  refocusing period should, therefore, be kept as small as possible (ideally  $< 15$  ms). This scheme has also been incorporated to the SeEXSIDE (SeEXSIDE\_PS, Figure S3) and EXSIDE (EXSIDE\_PS, Figure S4) experiments.

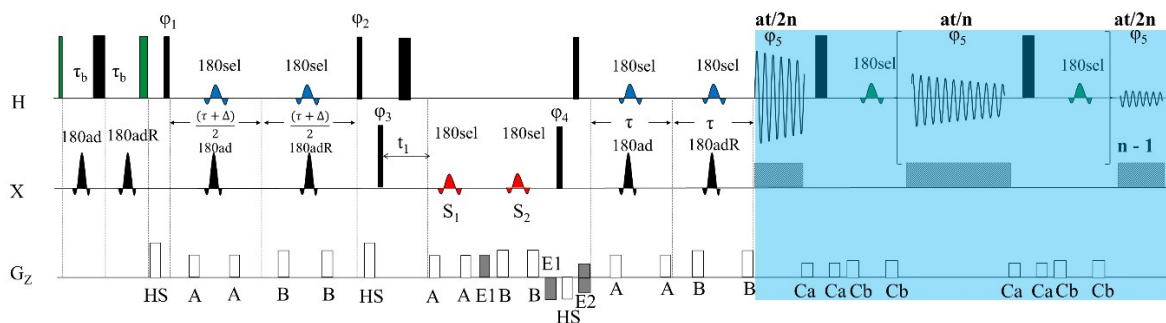


Figure S2: The ImpEXSIDE\_PS pulse sequence. Wide and narrow filled boxes represent  $180^\circ$  and  $90^\circ$  pulses respectively while thick and slim green boxes are  $135^\circ$  and  $45^\circ$  pulses respectively. Shaped pulses are  $^1\text{H}$  selective q3 (blue) and rsnob (green)  $^{13}\text{C}$  selective wurst2i (red) and broadband adiabatic (black) pulses. Delays are set thus;  $\tau = 1/(2 * {}^nJ_{CH})$ ,  $\tau_b = 1/(2 * {}^1J_{CH})$ , and  $\Delta = t_1 * J - scaling\ factor$ . Where  ${}^nJ_{CH} = 8\text{ Hz}$ ,  ${}^1J_{CH} = 146\text{ Hz}$  and  $J = 15$  in this instance. The phase cycle are;  $\phi_1 = x, x, -x, -x, -x, -x$ ,  $\phi_2 = y$ ,  $\phi_3 = x, -x$ ,  $\phi_4 = x, x, x, x, -x, -x, -x, -x$ ,  $\phi_5 = x, -x, -x, x, -x, x, x, -x$ . Pulses whose phases are not shown have an  $x$  phase. The pulse field gradients are shown in the  $G_z$  line as rectangular filled and unfilled boxes and coherence selection for desired  $^1\text{H} - ^{13}\text{C}$  correlation is achieved with 1.0 ms encoding/decoding gradients, E1:E2 whose power is set to 1.99:1 (1067:536.29 dB in this case). HS is a 1.0 ms homospoil gradient of power, 6180 dB which causes rapid relaxation of transverse magnetization present. Gradients 'A' and 'B' are 1.0 ms frequency dephasing/rephasing gradients of power 8531 and 1280 dB respectively whereas gradients 'Ca' and 'Cb' are 500  $\mu\text{s}$  long of power 250 and 375 dB respectively. The  $^{13}\text{C}$  band selective pulses,  $S_1$  and  $S_2$  (wurst2i pulses) can simultaneously and

efficiently excite multiple frequencies. The duration of the  $90^\circ$  pulse was  $9.8 \mu\text{s}$  (power, 58 dB) and  $9.0 \mu\text{s}$  (power, 54 dB) for  $^1\text{H}$  and  $^{13}\text{C}$  nuclei respectively. The adiabatic  $^{13}\text{C}$   $180^\circ$  pulse (denoted 180ad and 180adR) is a wurst2i swept pulse of duration  $465.5 \mu\text{s}$  and power 48 dB.

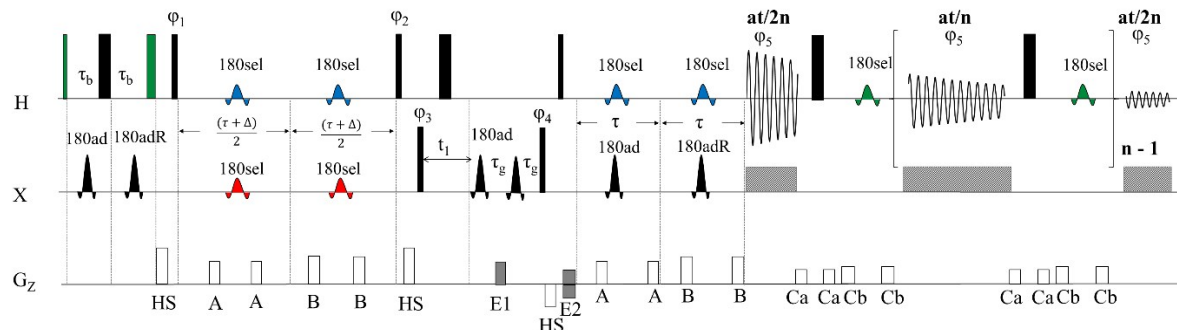


Figure S3: The SelEXSIDE\_PS pulse sequence. Wide and narrow filled boxes represent  $180^\circ$  and  $90^\circ$  pulses respectively while thick and slim green boxes are  $135^\circ$  and  $45^\circ$  pulses respectively. Shaped pulses are  $^1\text{H}$  selective q3 (blue) and rsnob (green),  $^{13}\text{C}$  selective wurst2i (red) and broadband adiabatic (black) pulses. Delays are set thus;  $\tau = 1/(2 * ^nJ_{CH})$ ,  $\tau_b = 1/(2 * ^1J_{CH})$ , and  $\Delta = t_1 * J - \text{scaling factor}$ . Where  $^nJ_{CH} = 8 \text{ Hz}$ ,  $^1J_{CH} = 146 \text{ Hz}$  and  $J = 15$  in this instance. The phase cycle are;  $\phi_1 = x, x, -x, -x$ ,  $\phi_2 = y$ ,  $\phi_3 = x, -x$ ,  $\phi_4 = x, x, x, x, -x, -x, -x, -x$ ,  $\phi_5 = x, -x, -x, x, -x, x, x, -x$ . Pulses whose phases are not shown have an  $x$  phase. The pulse field gradients are shown in the  $G_z$  line as rectangular filled and unfilled boxes and coherence selection for desired  $^1\text{H} - ^{13}\text{C}$  correlation is achieved with a 2.0ms (E1) and 1.0 ms (E2) encoding/decoding gradients, whose power ratio, E1:E2, is set to 1.99:1 (1067:536.29 dB in this case). HS is a 1.0 ms homospoil gradient of power, 6180 dB which causes rapid relaxation of transverse magnetization present. Gradients ‘A’ and ‘B’ are 1.0 ms frequency dephasing/rephasing gradients of power 8531 and 1280 dB respectively whereas gradients ‘Ca’ and ‘Cb’ are  $500 \mu\text{s}$  long of power 250 and 375 dB respectively. The duration of the  $90^\circ$  pulse was  $9.8 \mu\text{s}$  (power, 58 dB) and  $9.0 \mu\text{s}$  (power, 54 dB) for  $^1\text{H}$  and  $^{13}\text{C}$  nuclei respectively. The adiabatic  $^{13}\text{C}$   $180^\circ$  pulse (denoted 180ad and 180adR) is a wurst2i swept pulse of duration  $465.5 \mu\text{s}$  and power 48 dB.

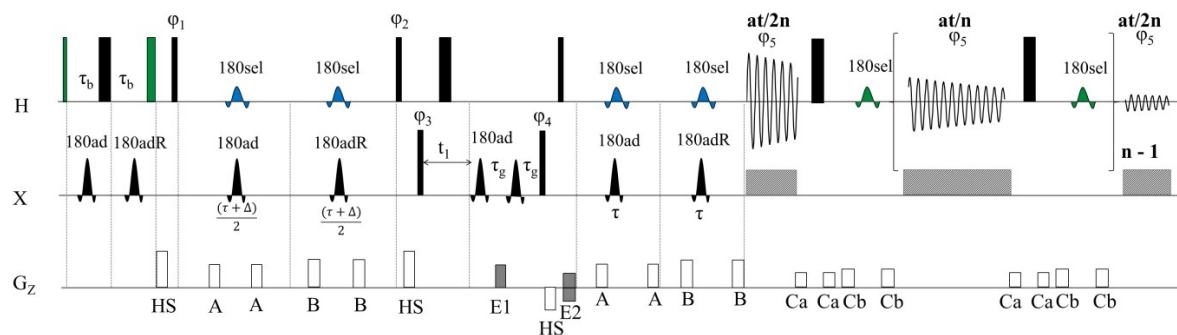


Figure S4: The EXSIDE\_PS pulse sequence. Wide and narrow filled boxes represent  $180^\circ$  and  $90^\circ$  pulses respectively while thick and slim green boxes are  $135^\circ$  and  $45^\circ$  pulses respectively. Shaped pulses are  $^1\text{H}$  selective q3 (blue) and rsnob (green) and  $^{13}\text{C}$  broadband adiabatic (black) pulses. Delays are set thus;  $\tau = 1/(2 * ^nJ_{CH})$ ,  $\tau_b = 1/(2 * ^1J_{CH})$ , and  $\Delta = t_1 * J - \text{scaling factor}$ . Where  $^nJ_{CH} = 8 \text{ Hz}$ ,  $^1J_{CH} = 146 \text{ Hz}$  and  $J = 15$  in this instance. The phase cycle are;  $\phi_1 = x, x, -x, -x$ ,  $\phi_2 = y$ ,  $\phi_3 = x, -x$ ,  $\phi_4 = x, x, x, x, -x, -x, -x, -x$ ,  $\phi_5 = x, -x, -x, x, -x, x, x, -x$ . Pulses whose phases are not shown have an  $x$  phase. The pulse field gradients are shown in the  $G_z$  line as rectangular filled and unfilled boxes and coherence selection for desired  $^1\text{H} - ^{13}\text{C}$  correlation is achieved with a 2.0ms (E1) and 1.0 ms (E2) encoding/decoding gradients, whose power ratio, E1:E2, is set to 1.99:1 (1067:536.29 dB in this case). HS is a 1.0 ms homospoil gradient of power, 6180 dB which causes rapid relaxation of transverse magnetization present. Gradients ‘A’ and ‘B’ are 1.0 ms frequency dephasing/rephasing gradients of power 8531 and 1280 dB respectively whereas gradients ‘Ca’ and ‘Cb’ are  $500 \mu\text{s}$  long of power 250 and 375 dB respectively. The duration of the  $90^\circ$  pulse was  $9.8 \mu\text{s}$  (power, 58 dB) and  $9.0 \mu\text{s}$  (power, 54 dB) for  $^1\text{H}$  and  $^{13}\text{C}$  nuclei respectively. The adiabatic  $^{13}\text{C}$   $180^\circ$  pulse (denoted 180ad and 180adR) is a wurst2i swept pulse of duration  $465.5 \mu\text{s}$  and power 48 dB.

The performance of the ImpEXSIDE and ImpEXSIDE\_PS sequences was further investigated using a more complex substrate, menthol and the sensitivity gains (signal:noise) are shown in Figure S5. We see approximately two-fold improvement in sensitivity when we compare the ImpEXSIDE\_PS data with those from ImpEXSIDE, while a sensitivity enhancement of up to 870 % (H1 – C6) is also observed when the ImpEXSIDE\_PS data is compared with the SeEXSIDE data. Moreover, signals too weak to be observed in the SeEXSIDE experiments, were measured with appreciable sensitivity in both the ImpEXSIDE and ImpEXSIDE\_PS experiments.

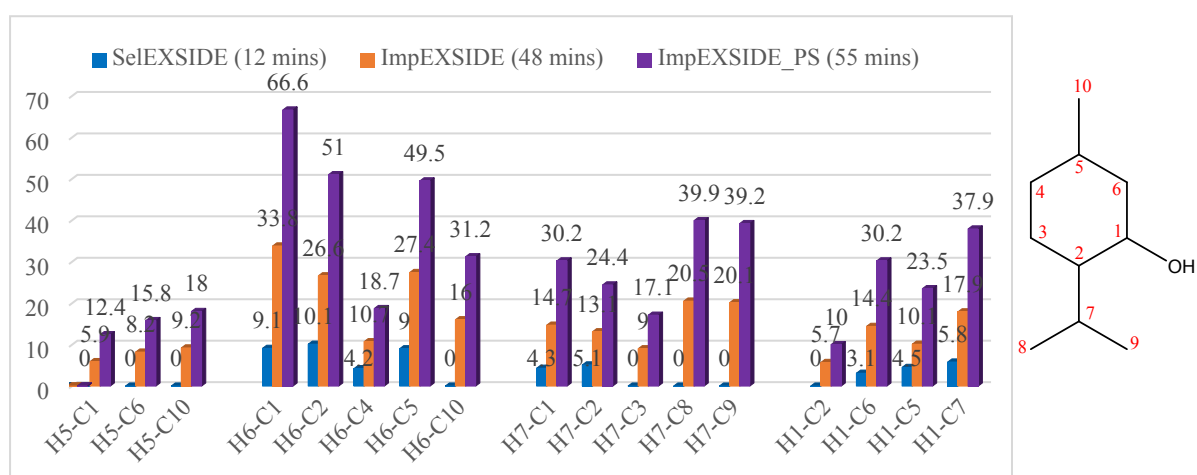


Figure S5: The signal to noise ratio of long range  $^1\text{H} - ^{13}\text{C}$  heteronuclear correlations of (-) menthol from bsEXSIDE (blue), ImpEXSIDE (orange) and ImpEXSIDE\_PS (purple) and structure of menthol.

## IMPRESS Acquisition and Processing

The ImpEXSIDE and ImpEXSIDE\_PS data shown in this paper were acquired with Hadamard encoding in an interleaved fashion using the Agilent (VNMRJ) format pulse sequence provided in the zipped file at the end of this supporting document. With this approach, the FID acquired per scan consists of four data sets of  $F_1$  complex points arrayed such that the phase modulation of the  $S_2$   $^{13}\text{C}$  selective pulse at the four chemical shifts, corresponds to the rows of the Hadamard matrix shown below with respect to each  $F_1$  data set acquired. Fourier transformation of this data in this form yields the convoluted aliased spectrum that cannot be easily interpreted. A processing macro (also provided in the zipped file) is then used to extract the desired spectrum using the appropriate sums/differences corresponding to the column of the same Hadamard matrix used. For instance, spectrum B (see  $H_4$  matrix below), is obtained with; ‘scan1-scan2+scan3-scan4’ whereas spectrum D will be the result of ‘scan1-scan2-scan3+scan4’.

$$H_4 = \begin{bmatrix} \text{Scan 1} & A & B & C & D \\ + & + & + & + & + \\ \text{Scan 2} & + & - & + & - \\ \text{Scan 3} & + & + & - & - \\ \text{Scan 4} & + & - & - & + \end{bmatrix}$$

Full details on how to implement and process the supplied pulse sequence and resulting data can be found in the Readme file enclosed in the zip file.

## An alternative approach to IMPRESS Acquisition and Processing

An alternative approach to collecting this data involves explicit acquisition, using the same set of parameters, of four separate spectra (i.e. running ‘4 spectra’ instead of ‘4 scans’) where the phase modulation of the  $S_2$  selective pulse at each of the chemical shifts of interest (A, B, C and D) is encoded in the manner of each row of the  $H_4$  Hadamard matrix above (see Figure S6). With this approach, four separate spectra are acquired with the pulse phases shown in Figure S6; (i)  $S_1 = S_{xxxx}$  and  $S_2 = S_{xxxx}$  (ii)  $S_1 = S_{xxxx}$  and  $S_2 = S_{xyyy}$  (iii)  $S_1 = S_{xxxx}$  and  $S_2 = S_{xxyy}$  (iv)  $S_1 = S_{xxxx}$  and  $S_2 = S_{xyyx}$ . Fourier Transformation of the four FIDs gives spectra with peaks in sites B, C and D aliased unto A but with phase properties corresponding to the phase of pulse  $S_2$  at their chemical shifts (note that the peak at A has the same phase property for all experiments as the phase of  $S_2$  at site A for all four experiments is ‘x’, corresponding to the first column of the  $H_4$  matrix). The desired peaks (with enhanced sensitivity) can then be extracted by a sum/difference of the four spectra using the appropriate columns of the  $H_4$  Hadamard matrix.

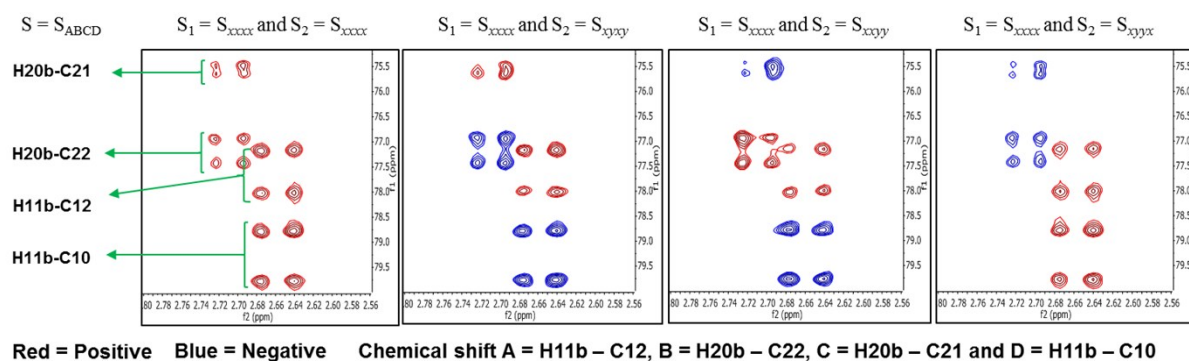
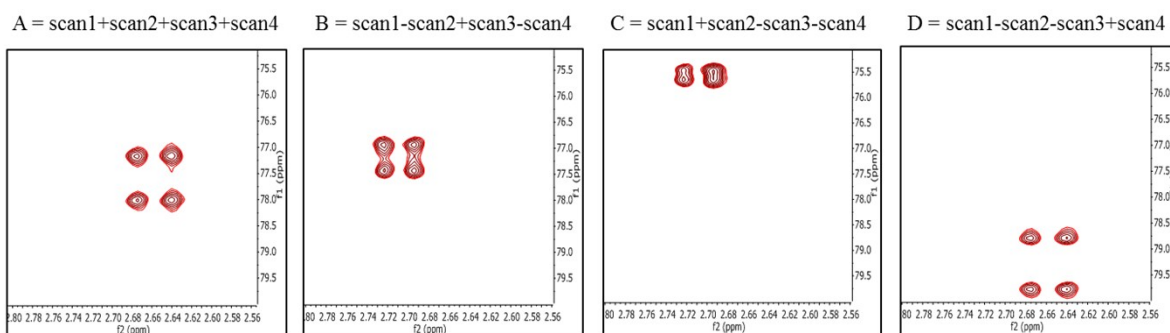


Figure S6: Figure showing the aliased peaks of the resonances (H11b – C12, H20b – C22, H20b – C21 and H11b – C10 of strychnine) at the four chemical shifts excited using the ImpEXSIDE sequence (Figure S1). These 4 separate spectra were acquired using the  $H_4$  Hadamard matrix shown above. The phase modulation of  $^{13}\text{C}$  selective pulses,  $S_1$  and  $S_2$  at the four chemical shifts A, B, C, and D are shown.



**Chemical shift A = H11b – C12, B = H20b – C22, C = H20b – C21 and D = H11b – C10**

Figure S7: The individual peaks obtained by appropriate sum/difference (shown above each spectra) of the four spectra of Figure S6.